



## **Anchorage capacity of corroded smooth reinforcement bars in existing reinforced structures.**

Downloaded from: <https://research.chalmers.se>, 2024-04-19 15:05 UTC

Citation for the original published paper (version of record):

Robuschi, S., Lundgren, K., Fernandez, I. et al (2018). Anchorage capacity of corroded smooth reinforcement bars in existing reinforced structures.. fib Symposium

N.B. When citing this work, cite the original published paper.

# Anchorage capacity of corroded smooth reinforcement bars in existing reinforced structures

Samanta Robuschi<sup>1</sup>, Karin Lundgren<sup>1</sup>, Ignasi Fernandez<sup>1</sup>, Kamyab Zandi<sup>1</sup>, Mathias Flansbjerg<sup>1,2</sup>.

*Department of Architecture and Civil Engineering, Division of Structural Engineering,  
Chalmers University of Technology,  
Sven Hultins gata 8, SE-412 96 Göteborg, Sweden*

*Division Safety and Transport, Mechanics Research,  
RISE Research Institutes of Sweden  
Brinellgatan 4, SE-504 62 Borås, Sweden*

## Abstract

Concrete structures are strongly affected by reinforcement corrosion, the most common cause of deterioration. Most studies on structural effects of corrosion rely on artificial methods to obtain a corrosion level that would otherwise require years, but doubts on the soundness of the methods have been raised. Specimens taken from existing structures offer the chance of studying the effect of natural corrosion, however the choice of the test setup is challenging. Hence, pilot tests are carried out to investigate the optimal design for testing the anchorage capacity of specimens with smooth reinforcements. The outcome is an asymmetrically supported 3-point bending beam test. The benefits of using complementary tools as Digital Image Correlation (DIC), Non-Linear Finite Element Analysis (NLFEA), pull-out tests and tensile tests and 3D scanning of the bars are presented.

## 1 Introduction

Nowadays, the need of properly assessing the structural capacity of existing structures is only foreseen to increase, as a result of the growing demand of load-carrying capacity and the aging of the structures themselves. Furthermore, the effects of climate change are likely to accelerate deterioration in the upcoming years, by anticipating the initiation of the corrosion process [1]. Corrosion is, indeed, the most common cause of deterioration [2]: chlorides penetration and carbonation are factors that lead to the depassivation of the reinforcements and, hence, to an increase of the corrosion risk.

Corrosion affects the structure in different ways [3]. Firstly, corrosion products occupy a larger volume than uncorroded steel: if no cracks are present in the specimen, it leads to an increase of the mechanical pressure on the bar that may increase the bond capacity by incrementing friction. On the other hand, an excessive amount of pressure can cause the cover to crack and spall. The properties of the bar itself are altered by the cross-section reduction and the changes in ductility. These phenomena affect the overall structural behaviour and decrease the safety of the structure.

Several studies on reinforced concrete structures with corroded ribbed bars can be found in literature. The same does not apply to structures with smooth bars: the use of this kind of bars drastically diminished from the 40s to nowadays, yet, several structures are still standing and subject to increasing demands of load-carrying capacity, as well as most likely damaged by corrosion.

The bond between reinforcements and concrete is commonly studied as a result of three mechanisms: chemical adhesion, friction and mechanical interlocking between the ribs and the concrete. In the case of smooth bars, mechanical interlock acts on a micro-level, between the concrete and the imperfection in the reinforcement shape. Sliding friction [4], as to indicate the wedging action of small particles of concrete detached by the initiation of the slip, contributes to the mechanical interlock.

The bond capacity of smooth bars is naturally lower than the one of ribbed bars. The presence of corrosion products noticeably affects the bond properties by increasing the normal stresses on the bar, and therefore friction [3] [5]. Corrosion would as well influence the sliding friction mechanism.

The casting position is a parameter that additionally influences the bond of smooth bars: top-cast bars are more likely surrounded by a less dense concrete, leading to a smaller bond capacity for top-

cast than for bottom-cast bars. This effect is more pronounced for smooth bars than for ribbed. Furthermore, smooth bars generate less splitting stresses, due to the absence of ribs.

Few publications can be found in literature combining smooth bars and corrosion. Recent studies by Cairns et al. [5] [6] investigate the bond behaviour of smooth bars when subjected to artificial corrosion, but several uncertainties still stand on how well this can represent the corrosion process in real structures. Hence, existing structures offer a unique opportunity to study the effects of natural corrosion on specimens affected by aging processes that are typical of concrete structures, as shrinking and creep, as well as built with the actual materials used in the past.

The choice of a test set-up for the study of the anchorage capacity of an existing structure presents some challenges, since the material properties, the amount of reinforcement and the geometry of the cross section are given. Furthermore, geometrical properties, such as concrete cover and stirrup spacing, are likely to vary from specimen to specimen and the identification of the reinforcement could itself be a challenge, if the structure highly differs from the original drawings.

The aim of this study is to design a test set-up for investigating the anchorage capacity of smooth bars affected by corrosion in a large experimental campaign: specimen coming from Gullspång bridge (Sweden) will be tested to provide further knowledge on the topic.

## 2 Methodology

### 2.1 Methods

The study can be divided in two main phases:

- a preliminary phase, in which data from literature was collected, and Finite Element (FE) and analytical analyses of possible test setups were done;
- a pilot study, where three test setups were selected and tested.

Finally, the test setup for the experimental campaign was chosen by analysing and comparing the results of the pilot study.

### 2.2 Specimens

Gullspång bridge was built in 1935 and torn down in 2016 due to heavy corrosion damages. The edge beams were carefully taken out, cut in segments and designated to be used for research. Having been exposed for 81 years to weather conditions that include snow, icing cycles and wind, as well as to de-icing salts and traffic loads, the beams present different cracks on their surface, and spalling strongly affects the geometry in some locations (Fig. 1). Signs of corrosion are clearly visible, but not uniformly distributed: the varying level of degradation offers the possibility to study an existing structure with its natural scatter.

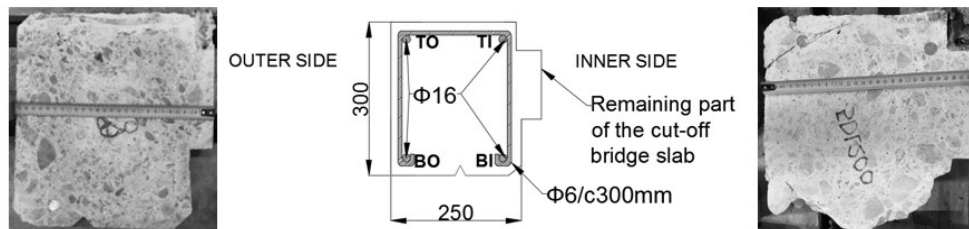


Fig. 1 Two different cross sections of the edge beams as positioned on the bridge are shown, together with the geometry of the cross section (according to the original drawings): the remaining part of the cut-off bridge slab is clearly visible to the right. Dimensions in mm.

The edge beams are characterized by  $\Phi 6$  stirrups, open on the bottom side with respect to the original position on the bridge, and by 4  $\Phi 16$  smooth reinforcement bars, two at the top and two at the bottom of the cross section, with varying concrete cover (3.4 cm according to the original drawings). The cross section is 300x250 mm, with approximately 50 mm of cut-off from the bridge slab sticking out on the inner side (Fig. 1). The geometry of the beam itself is far from perfect: the space between the stirrups was according to drawings 300 mm, but a great variability in the actual distance could be observed.

Cracks and differences in geometry were carefully inspected and documented. The material properties were affected by the aging of the structure, and therefore the specification from the original drawings cannot be fully trusted. In a field survey done 1988, the concrete compressive strength was measured to about 45 MPa, while the yield strength of the smooth reinforcement bars was measured to about 252 MPa. The steel bars well represent the material of the time of construction, when it was common to have low yield strength and anchorage was achieved by means of bending the bars in hooks. To reach a more comprehensive understanding of the material properties, further material tests are planned.

### 3 Design of the test set-up

#### 3.1 General design requirements

To investigate the test setup that would best apply to Gullspång specimens, the following general design requirements were established:

- The test setup should have high chance to reach anchorage failure;
- the test setup should be simple and easy to apply to specimens from existing structures;
- the bond should be disturbed as little as possible by external factors;
- the test setup should have clear boundary conditions, thus making it easier to compare the experimental results with a FE model;
- the test setup should allow for testing both bottom cast and top cast bars.

These principles were taken into consideration all through the different phases of the design process.

#### 3.2 Preliminary phase

In literature, pull-out tests and beam tests are the most commonly used test methods when dealing with specimens affected by corrosion: while beam tests have been employed for both newly cast and existing structures [7], pull-out tests have been used to investigate the local bond capacity only for newly cast specimens, corroded artificially [6] [8].

ACI committee 408 [9] argues that splice and beam-end specimens best replicate the stress state in concrete when testing the bond capacity of flexural members, but substantial modifications to the geometry of the beams would be needed to perform such tests on Gullspång bridge specimens, thus possibly affecting the bond.

The first setup to be considered was an indirectly supported 4-point bending test, as previously adopted in the evaluation of the bond capacity of corroded existing concrete structures with ribbed bars [7]. The test setup has been designed to reach anchorage failure after the opening of a major shear crack, and indirect supports have been employed to avoid adding external pressure on the reinforcement bars, thus making it easier to analyse the test results without the risk of estimating an increased bond capacity. The use of indirect supports, on the other hand, leads to the need of drilling holes in the specimens and, consequently, strengthening to avoid local failure. These measures were considered too complicated to carry out for the excessively damaged beams in this project; they had severe spalling and diffuse cracking of concrete.

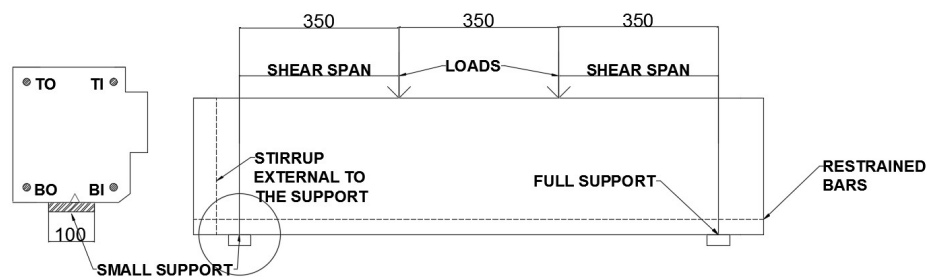


Fig. 2 Directly supported 4-point bending test setup. Dimensions in mm.

The next considered test setup consisted, therefore, of a directly supported 4-point bending beam test, where both supports and boundary conditions were asymmetric (Fig. 2). To directly support the beam while minimizing support pressure on the reinforcements, a narrow support was introduced, positioned in between the bars and used on one side of the beam where anchorage failure was expected. The specimen was designed to have a stirrup external to the small support to help redistribute the higher concentrated stresses generated by the support. On the other side, where a full support was to be used, the ends of the bars were restrained by means of washers and bolts to avoid slips.

The 4-point bending test setup was designed by means of analytical calculations and FE analyses (Fig. 3). The anchorage length was compared to the yield strength of the bar, with the aim of avoiding yielding of the bars, as in (1):

$$2\pi r \cdot \tau_b \cdot l_a = f_{y,s} \pi r^2 \quad (1)$$

where  $\tau_b$  is the average bond stress,  $l_a$  is the available anchorage length,  $r$  is the radius of the bar while  $f_{y,s}$  is the average yield strength (252 MPa). The bond is evaluated as uniformly distributed along the anchorage length. By plotting the bond as a function of the anchorage length, it became clearly visible that the anchorage length was remarkably limited by the yield strength of the bars, if yielding was to be avoided (Fig. 3). It was, as well, clear that in case of high bond stresses, the test would be affected by yielding.

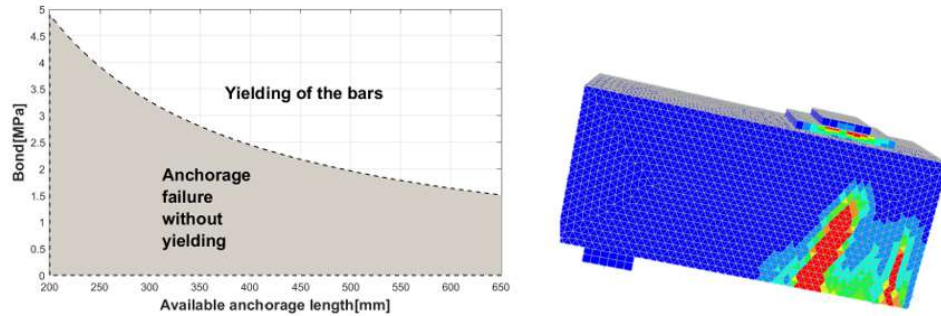


Fig. 3 To the left, the bond capacity needed to reach yielding for a given anchorage length. To the right, the crack pattern of the 4-point bending test resulting from an FE analysis.

The FE analyses were performed using the commercial software Diana 10.0 [10]. To decrease computational time, only half of the specimen was modeled, with the aim of focusing on the small support side. Concrete elements were modelled with 3D tetraedral elements, a constitutive model based on non-linear fracture mechanics and a smeared crack approach based on a total-strain crack model. Thorenfeldt compression function and Hordijk tensile curve were used in characterizing concrete. A bond-slip relationship combined with embedded reinforcement approach was employed to represent the bond behaviour of the smooth bars, while the material properties of the steel were described by an elastoplastic material model without hardening. The bond capacity was varied between 1 and 7 MPa. Both the support and the load plate were modelled by means of a steel plate and a wooden board. The load was applied by means of displacement control on the top of the steel load plate.

The aim of the analyses was to investigate the crack pattern: when designing a test that would result in anchorage failure, the anchorage length should be short enough to allow the bars to start slipping before any other ultimate failure would occur; i.e. shear failure, crushing of concrete or rupture of the reinforcements. It was observed that:

- the low bond capacity of smooth bars, together with the low reinforcement ratio (0.54%) and the low yield strength makes it difficult for the beam to redistribute stresses after opening of the first bending cracks; no shear crack was observed in the analyses, bending cracks would instead open either underneath the loading plates or in the mid-span (Fig. 3, right);
- yielding of the bars follows shortly after reaching the cracking moment;
- the opening order and the position of the bending cracks could not be predicted since it is likely to depend on the variation of the material and geometrical properties in the beams.

A second test setup, that would allow for a shorter anchorage length, was hence introduced: a directly supported 3-point bending beam test, with the same asymmetric supports and boundary conditions as the first alternative (Fig. 5). By removing the constant bending moment span, the crack pattern is more likely to be characterized by a single bending crack, which would appear underneath the load plate, where the cross section subjected to the maximum moment is located. FE analysis and analytical calculations were once again employed to choose the shear span and to investigate the crack pattern.

In both test setups, it was chosen to adopt a shear span 5 cm longer than the height of the beam, to reduce the anchorage length of the bars to a minimum while avoiding characterizing the entire shear span as a discontinuity region: the span was initially of 350 mm for both the tests. Even in this case, it was observed that only a small bond capacity would avoid yielding of the bars. To avoid cutting through a steel plate positioned on the side of the specimen, once used for connecting the railings of the bridge to the edge beams, the shear span of the 3-point bending beam had to be extended with 1.5 cm (Fig. 4).

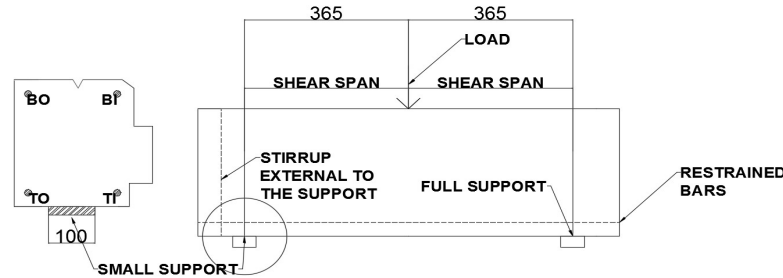


Fig. 4 Directly supported 3-point bending test set-up. Dimensions in mm.

### 3.3 Pilot study

Three tests were carried out in the context of the pilot study:

- Test 1 was an asymmetrically supported 3-point bending test (Fig. 4), with bars restrained on one side, tested upside-down with respect to the original position on the bridge; this resulted in anchorage failure;
- Test 2 was an asymmetrically supported 4-point bending test, with bars restrained on one side, tested upside-down with respect to the position on the bridge; this presented signs of anchorage failure on the restrained side;
- Test 3 was an asymmetrically supported 4-point bending test, with no bars restrained, tested as positioned on the bridge; this resulted in anchorage failure, but on the full support side (Fig. 2).

During the pilot study, the optimal solution for monitoring the tests was, additionally, investigated by adopting different methods. The first test was completely monitored with LVDTs: two LVDTs moved together with the bars on the small support side, via a magnetic connection, where they measured the relative slip of the bar against the concrete surface, while four LVDTs were employed for monitoring the support settlements, by measuring the vertical displacement of steel angles glued over the supports. Lastly, a LVDT measured the mid-span deflection.

In the second test, Digital Image Correlation was used to capture the front view of the specimen, thus acquiring data on the deflection of the specimen and the opening of the cracks. LVDTs were still used to monitor the slips of the bars, the mid-span deflection and the support settlements on the back side of the beam. In the last test, however, support settlements were as well measured with DIC, and only the bar slips and the mid-span deflection were monitored with LVDTs; the latest measure to be used as a mean of comparing the results from the two different methods.

## 4 Results and discussion

### 4.1 Directly supported 3-point bending

The 3-point bending test was characterized by the opening of a major bending crack, followed by yielding of the bars and finally by slip of the bars on the small support side; one bar at a time started to slip (Fig. 5).

The average maximum bond stress was estimated by assuming that both bars were carrying the same force at the maximum applied load, and a constant bond stress along the available anchorage length:

$$\bar{\tau}_{b,max} = \frac{F_t}{s_h} = \frac{M}{0.9 \cdot d} \cdot \frac{1}{2\pi r \cdot l_a \cdot 2} = \frac{P \cdot l_s}{8 \cdot 0.9 \cdot d \cdot \pi \cdot r \cdot l_a} = 3.17 \text{ MPa}, \quad (2)$$

where  $F_t$  is the tensile force in the bars,  $M$  is the moment generated by the maximum load  $P$ ,  $l_s$  is the shear span,  $s_h$  is the bond surface,  $d$  is the effective height of the section and  $r$  is the radius of the reinforcement bars. The available anchorage length,  $l_a$  is evaluated as the distance of the crack from the edge of the beam. It should be noted that when the maximum load was reached, yielding was already taking place in the bars; the actual bond capacity of the bars was therefore likely higher than the evaluated, as the loss of bond in the yield penetration zone is not taken into account. A better estimation of the yield penetration will be possible after 3D scanning of the bars.

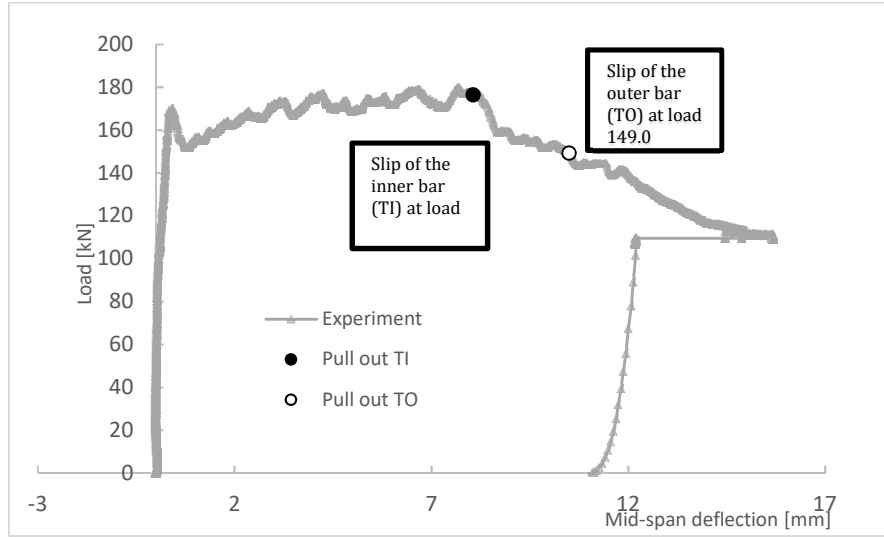


Fig. 5 Results from the directly supported 3-point bending test: load versus mid span deflection.

The two reinforcement bars started to slip at different times (Fig. 5). The first bar, that was originally positioned on the Top Inner part of the bridge (TI) (Fig. 1), started to slip shortly after the reaching the maximum load, while the second one (Top Outer part of the bridge) followed the first after 5.5 mm. A first visual inspection showed that the level of corrosion of the two bars was different: the first bar to slip (TI) presented only small signs of corrosion, while the second one (TO) was more heavily corroded. The estimated elongation of the bars differed as well, being about 3% for TI and 4% for TO. By assuming the load to be evenly distributed, the stresses in each bar at the maximum load resulted in 349.5 MPa, which is reasonable for the estimated elongation of the bars when compared to the results of the tensile tests of the bars.

It was observed that by acquiring data on the crack pattern on the front side of the beam, the anchorage length would be better estimated: this led to the introduction of DIC as a mean of monitoring the beams in the following tests.

## 4.2 Directly supported 4-point bending

Monitoring the front side of the beam by means of DIC made it possible to gain more knowledge on the specimen behaviour, by acquiring data on the crack distance and crack opening development. The major strains captured by the cameras clearly showed the opening of the cracks before they were visible to the naked eye (Figs. 6-7).

In both tests, cracks localized in three different locations: underneath the load plates and in the mid-span. During the first 4-point bending test, only the crack in the mid span and the one close to the full support continued to open (the latter located at a cast joint). The opening of the two cracks was followed by yielding and, afterwards, by failure of the beam on the full support side, where the slip of the restrained bars bent the washers. Given the outcome of the first test, it was observed that restraining the bars at the side with full support was likely to lead to a high percentage of tests with no anchorage failure in a 4-point bending test, due to the uncertainty in the crack pattern. It was therefore chosen, in the second test, not to use restraints on the side with the full support, but to monitor the slips on both sides.

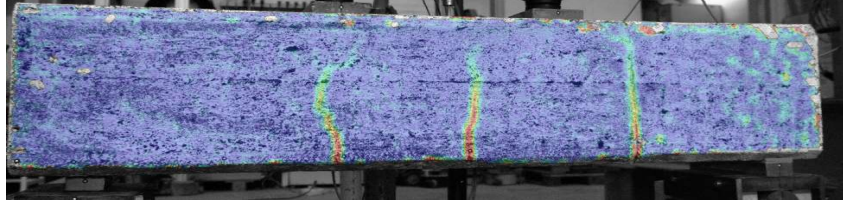


Fig. 6 Directly supported 4-point bending, second test: strain concentrations after cracking. Crack distance (from left): 190 mm-269 mm.

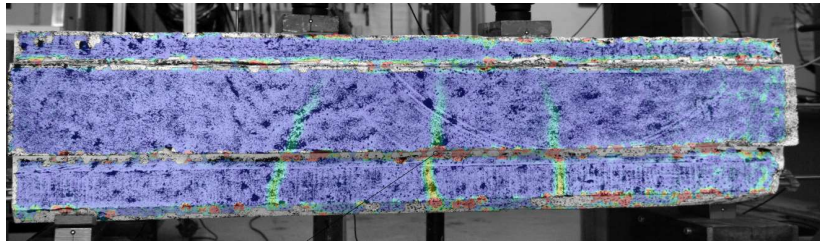


Fig. 7 Directly supported 4-point bending, third test: strain concentrations after cracking. Crack distance (from left): 240 mm-211 mm.

The third test (Fig. 7) was characterized by the development of the two cracks underneath the load plates. Yielding of the bars followed and slipping of the bars started, one at a time, after 15 mm of mid-span deflection. The bar positioned internally in the original bridge (Bottom Inner) started to slip first, on the full support side, though the available anchorage length on the full support side was only 25 mm shorter than on the other side. After further crack development, the beam started to tip, and ultimately collapsed on the floor when the second bar (Bottom Outer) suddenly slipped 1 mm on the full support side.

## 5 Conclusions

The results from the 4-point bending tests clearly show that the test setup is not well suited for testing the anchorage capacity of the edge beams of Gullspång bridge: in the two pilot cases, the cracks developed in different order and positions, meaning that the anchorage length would strongly vary between different tests, which would complicate the evaluation of the results.

The 3-point bending test, on the other hand, gave results easier to evaluate, provided that the necessary complementary tools are used in the interpretation, such as analysing the steel bars, and using DIC measurements for capturing the crack opening.

The latest two tests showed that:

- Restraining the bars on the full support side does not prevent anchorage failure when the anchorage length is significantly smaller on that side (second test);
- the presence of a full support does not increase the bar confinement enough to prevent anchorage failure on the full support side when the bars are not restrained (third test).



These preliminary considerations are likely to be affected by different factors, such as the presence of spalling cracks prior testing and differences in the concrete cover or on the corrosion level. Given these observations it was nevertheless chosen not to use restraints on the full support side. The asymmetric support conditions will be kept though, to observe the influence of support pressure on the bond capacity.

As a result of this study, the bond between concrete and smooth reinforcement bars will be investigated by means of asymmetrically directly supported 3-point bending tests. Furthermore, the importance of acquiring data on the corrosion level and the yield penetration by means of 3D scanning and tensile tests of the reinforcement bars is highlighted.

The tests will be monitored by use of LVDTs to measure the end slips of the bars, and DIC to acquire data on the crack pattern and opening, and the displacements of the beam.

The need of a simple test setup is strongly enlightened by the results of the pilot study. Existing structures are, in fact, subjected to a great variability of material and geometrical parameters, and the test setup needs to be able to produce comparable results.

Further knowledge on the material parameters will be needed to fully assess the results from the beam tests: the use of the single beam test is not able to guarantee enough understanding of the bond capacity of smooth bars. In particular, data on the local bond-slip, when not affected by yielding of the reinforcement bars, is needed to fully characterize the bond: pull-out tests of bars with varying anchorage length (5, 7.5 and 10 cm) are therefore introduced in the experimental campaign. Since the use of reinforcement bars with low tensile strength is common in old structure, it is considered valuable to include the effect of yielding on bond.

In future work, the use of Finite Element Modelling coupled to experimental results is seen as a possible solution for overcoming the test setup limitations and avoid wrong conclusions, such as a higher bond capacity due to the support pressure in beam tests or to the compressing stresses impressed to the concrete in the pull-out tests [11]. Furthermore, the swelling action of the corrosion is to be included in the modelling and a frictional model for the bond is to be calibrated.

## References

- [1] Wang, Xiaoming, Stewart, Mark G., and Nguyen, Minh. 2012. "Impact of climate change on corrosion and damage to concrete infrastructure in Australia." *Climate Change*, 110(3-4):941-957.
- [2] Bell, B. 2004. Sustainable bridges. D1.3 *European Railway Bridge Problems*.
- [3] Lundgren, K. 2007. Effect of corrosion on the bond between steel and concrete: an overview. *Magazine of Concrete Research*, 59(6):447-461.
- [4] Abrams, D. 1913. Test of bond between concrete and Steel. *PhD Thesis, Urbana University of Illinois*.
- [5] Cairns, J., Du, Y., and Law, D. 2008. Structural performance of corrosion-damaged concrete beams. *Magazine of Concrete Research*, 60(5):359-370.
- [6] Cairns, J., Du, Y., and Law, D. 2006. Residual bond strength of corroded plain round bars. *ConRes*, 58(4):221-231.
- [7] Tahershamsi, Mohammad, Kamyab, Zandi, Lundgren, Karin, and Plos, Mario. 2014. Anchorage of naturally corroded bars in reinforced concrete structures. *Magazine of Concrete Research*, 66(14):729-744.
- [8] G. Berrocal, Carlos, Fernandez, Ignasi, Lundgren, Karin, and Löfgren, Ingemar. 2017. Corrosion-induced cracking and bond behaviour of corroded reinforcement bars in SFRC. *Composites, Part B: Engineering*, 113:123.
- [9] ACI Committee 408. 2003 ACI 408R-03. Bond and Development of Straight Reinforcing Bars in Tension. *American Concrete Institute*, 1-49.
- [10] DIANA, User's Manual, release 10.1, 2016. DIANA FEA BV, Delft, the Netherlands.
- [11] Cairns, J., and Plizzari, G.A. 2003. Towards a harmonized European bond test. *Materials and Structures*, 36:495-506.